



Article

A test of Amati relation using HII galaxy distances

Rikiya Okazaki¹ and Shantanu Desai^{2,*}

- Department of Mathematical Engineering and Information Physics, The University of Tokyo, Tokyo, Japan; r.okazaki663@gmail.com
- Department of Physics, IIT Hyderabad, Kandi, Telangana-502284, India; shntn05@gmail.com (S.D.)
- * Correspondence: shntn05@gmail.com

Abstract: We use model-independent luminosity distances of 186 HII galaxy observations to address the circularity problem in the Amati relation for Gamma-ray Bursts (GRBs). For this purpose, we used Artificial Neural Network based interpolation to reconstruct the luminosity distance corresponding to the GRB redshift. We then use two independent GRB datasets to test the robustness of the Amati relation at redshifts below z=2.6. Our best-fit Amati relation parameters are consistent for the same datasets to within 1σ . The intrinsic scatters which we obtain for the two datasets of about 28% and 35%, are comparatively larger. This implies that the Amati relation using HII galaxies as distance anchors cannot be used as a probe of precision cosmology.

Keywords: Gamma-Ray bursts; Amati Relation; HII Galaxies

1. Introduction

Gamma-ray bursts (GRBs) are short-duration single-shot events, which have been detected over a broad range from keV to TeV [1]. They are broadly classified into two categories: short and long, depending on whether their duration is less than or greater than two seconds [2]. Long-duration GRBs have been associated with core-collapse supernova [3], while short GRBs are associated with binary neutron star mergers [4]. However, there are a large number of exceptions to this general rule [5] (and references therein).

For more than two decades, GRBs have also been proposed as standard candles using observed correlations between different GRB observables [6–12]. Among these, the most widely studied correlation is the Amati relation, which posits a tight relation between the spectral peak energy in the GRB rest frame and the equivalent isotropic radiated energy [13,14]. However, because of the scarcity of GRBs at low redshifts, the Amati relation can only be probed after assuming a cosmological model [6,9,15].

To avoid the aforementioned circularity problem, two methodologies have been used in the literature. The first approach is to simultaneously constrain both the cosmological model parameters and the Amati correlation parameters [16–20]. Alternately, a number of ancillary probes have also been used to get model-independent estimates of distances corresponding to the GRB redshift, such as Type 1a SN [21–26], Cosmic chronometers [27–33], Baryon Acoustic Oscillation H(z) measurements [30], galaxy clusters [34], X-ray and UV luminosities of quasars [35]. In a similar vein, we use the HII galaxy distances to study the efficacy of the Amati relation, without relying on an underlying cosmological model.

HII galaxies are compact galaxies undergoing intense episodes of star formation. The H β luminosity for these galaxies has been found to be strongly correlated with the ionized gas velocity dispersion ($\sigma(H\beta)$) with negligible scatter [36]. Therefore, observations of the H β flux ($F(H\beta)$) for these galaxies can be used as model-independent probes of



Received: Revised:

Accepted: Published:

Citation: . Title. *Universe* **2025**, *1*, 0. https://doi.org/

Copyright: © 2024 by the authors. Licensee MDPI, Basel, Switzerland. This article is an open access article distributed under the terms and conditions of the Creative Commons Attribution (CC BY) license (https://creativecommons.org/licenses/by/4.0/).

Universe **2025**, 1, 0 2 of 9

cosmic expansion [37–39]. Most recently, they have been used to compare the $R_h = ct$ cosmological model with the Λ CDM [40] and a test of cosmic distance duality relation [41]. The luminosity distance (D_L) and distance modulus (μ) can be obtained from HII galaxy observables ($\sigma(H\beta)$ and $F(H\beta)$) as follows [41] (and references therein):

$$\mu = 5\log_{10}\left(\frac{D_L}{\text{Mpc}}\right) + 25 = 2.5\left[\alpha\log_{10}\left(\frac{\sigma(H\beta)}{\text{km s}^{-1}}\right) - \log_{10}\left(\frac{F(H\beta)}{\text{erg s}^{-1}\text{ cm}^{-2}}\right) + \beta\right] - 100.2,$$
(1)

where α and β are empirical constants characterizing the slope and intercept of the regression relation between H β luminosity and $\sigma(H\beta)$. The constants (α and β) have been shown to be agnostic to the underlying cosmological model. We use the values $\alpha=33.72\pm0.12$ and $\beta=4.64\pm0.10$ [40]. The luminosity distance to the GRBs is then obtained using the above distances to HII galaxies as anchors.

This manuscript is structured as follows. We describe the GRB and HII galaxy data used for our analysis in Sect. 2. Our results are discussed in Sect. 3. We conclude in Sect. 4.

2. Datasets

2.1. GRB data

The GRB datasets used in our analysis are the same as those used in [34] (G22, hereafter) and also [35]. The first dataset (referred to as A220 dataset [18]), consists of 220 long GRBs spanning the redshift range $0.0331 \le z \le 8.20$ [18]. For this dataset, the redshift, peak GRB energy in the rest frame (E_p), and GRB bolometric fluence (S_{bol}) have been provided. The second data set (referred to as the D17 data set) [24,42] consists of 162 long GRBs in the redshift range $0.125 \le z \le 9.3$. For this data set, GRB redshift, distance modulus (using Type Ia Supernovae as anchors), E_p , and E_{iso} have been provided. For both these datasets, 1σ uncertainties are provided for each of the observables.

2.2. HII galaxy data

The HII galaxy data set we considered for this analysis consists of a sample of 195 sources. This includes a sample of 181 HII galaxies (HIIGx) in the redshift range 0.01 < z < 2.6 [43] and 14 newly discovered HIIGx samples [44,45], including 5 from JWST. The redshift range of the entire sample spans $0.0088 \le z \le 7.43$. However, there are very few sources located beyond redshift of 2.6. Therefore, we restrict our analysis upto a maximum redshift z = 2.6, which yields a total of 186 HII galaxy distances.

3. Analysis and Results

The Amati relation can be written as a linear regression relation between the logarithm of isotropic equivalent energy (E_{iso}) and GRB peak energy in the rest frame (E_p):

$$y = ax + b \tag{2}$$

where $y \equiv \log(E_p(keV))$ and $x \equiv \log(E_{iso}(erg))$. Note that E_p is related to the GRB peak energy in the observer frame given by $E_p = E_p^{obs}(1+z)$. E_{iso} is related to the bolometric fluence (S_{bolo}) according to:

$$E_{iso} = 4\pi d_I^2 S_{hol} (1+z)^{-1}, (3)$$

The next step in the analysis involves obtaining a model-independent estimate of D_L from HII galaxy observables from Eq. 1. We then need to reconstruct D_L at any intermediate redshifts. For this purpose, we use Artificial Neural Networks (ANN), a non-parametric regression technique widely used in Astrophysics [46]. A summary of other interpolation methods used for calibrating the Amati relation and comparisons with ANN can be found

Universe **2025**, 1, 0 3 of 9

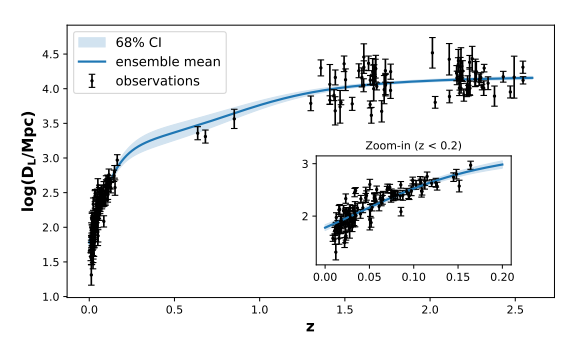


Figure 1. Non-Parametric reconstruction of D_L using ANN-based regression from HII Galaxy measurements upto z of 2.6. The blue shaded region shows the 68% allowed region.

in [26]. The ANN consists of an input layer, multiple hidden layers, followed by an output layer. During each layer, a linear transformation is applied to the input vector from the previous layer followed by a non-linear activation function (a simple mathematical operation that enables the network to learn complex, non-linear relationships), which then gets propagated to the next layer. For our analysis, we use the Sigmoid activation function for all hidden layers and the identity function for the output layer. The network is implemented using pytorch. To perform the regression while robustly accounting for both the uncertainty arising from our finite sample size and the uncertainty propagated from individual measurement errors, we employed ensemble learning based on bootstrapping and data perturbation [47], as explained below. We trained K independent ANNs. The training set for each k-th network, S'_k , was generated as follows:

1. A bootstrap sample S_k was drawn with replacement from the original dataset

$$S = \left\{ \left(z^i, \log D_L^i, \sigma_{\log D_L}^i \right) \right\}_i$$

, where $\sigma^i_{\log D_L}$ denotes the standard deviation of $\log D^i_L$

2. A perturbed dataset S'_k was created by sampling new target values $(\log D_L^j)'$ for each point $(z^j, \log D_L^j, \sigma^j_{\log D_L})$ in S_k from a Gaussian distribution reflecting its measurement error:

$$(\log D_L^j)' \sim \mathcal{N}(\log D_L^j, (\sigma_{\log D_L}^j)^2)$$

Each ANN was then trained on its unique dataset S_k' . For any new input z, the final predicted value $\log D_L(z)$ is the mean of the K network outputs, and the total propagated uncertainty $\sigma_{\log D_L}(z)$ is its standard deviation. The hyperparameters (structural settings of the model determined prior to training, such as the learning rate or the number of hidden neurons) were determined through cross-validation before the learning. The ANN therefore enables us to reconstruct D_L at any redshift z. This reconstructed value of z0 upto redshift of 2.6 can be found in Fig. 1. Beyond redshift of 2.6, we have very few HII galaxies, making it difficult to do the interpolation and hence we ignore these galaxies.

The ANN-based interpolation described above allows us to reconstruct D_L for both the A220 and D17 GRB dataset. We then re-estimate E_{iso} using Eq. 3 and then carry out the

Universe **2025**, 1, 0 4 of 9

analysis for the Amati relation. To calculate the best-fit parameters of the Amati relation, we use Bayesian regression and maximize the same likelihood as that in G22:

$$-2\ln L = \sum_{i} \ln 2\pi \sigma_i^2 + \sum_{i} \frac{[y_i - (ax_i + b)]^2}{\sigma_i^2 (a^2 + 1)}$$
 (4)

$$\sigma_i^2 = \frac{\sigma_{y_i}^2 + a^2 \sigma_{x_i}^2}{a^2 + 1} + \sigma_s^2 \tag{5}$$

 σ_x and σ_y denote the errors in $\log(E_{iso})$ and $\log(E_p)$, obtained using error propagation; and σ_s denotes the intrinsic scatter, which characterizes the tightness of the relation. We used the same priors as those in G22, consisting of uniform priors on a and b, and log-uniform priors on σ_s : $a \in [0,1]$, $b \in [-30,-10]$, $\sigma_s \in [10^{-5},1]$. We sample the likelihood using the emcee MCMC sampler [48].

The marginalized 68% and 95% credible interval plots for the Amati relation parameters along with the intrinsic scatter can be found in Fig. 2 and Fig. 3 for the D17 and A220 GRB datasets, respectively. The scatter plots for E_p versus E_{iso} along with the best-fit Amati relation for A220 and D17 dataset can be found in Fig. 4 and Fig. 5, respectively. A tabular summary of our results can be found in Table 1.

For the A220 dataset, the best-fit value of a is equal to 0.54 ± 0.02 with an intrinsic scatter of 28%. The best-fit value of a is consistent with that obtained in G22 to within 1σ . This scatter is smaller than the scatter of around 45% obtained in G22 (for z < 0.9) and [18], or the value of 50% obtained in [49].

For the D17 dataset, we find $a = 0.4 \pm 0.03$ with an intrinsic scatter of 35%. The best-fit value of a is again consistent with that obtained in G22 to within 1σ . The scatter obtained in this work, however, is substantially larger than the value of 15% obtained in G22 (for z < 0.9) or the value of 26% obtained using quasars in [35] (for $z \le 1$).

Recent analysis of the Amati relation have found much larger scatter compared to the two datasets we have analyzed. A scatter of 39% was obtained from a joint fitting of the cosmology and Amati relation [19]. A subsequent analysis by the same group found a scatter of 55% - 65% using an updated GRB dataset [20]. Using cosmic chronometers as distance anchors for a sample of long GRBs from Fermi-GRB, an intrinsic scatter of 50-65% was obtained for $z \le 1.4$ [32] and 41-59% for z < 1.2 or z < 1.965 [33].

Therefore, we find that although the Amati slope is consistent with previous results, which used disparate external observables as distance anchors, the intrinsic scatter using the HII galaxies as distance anchors is still very large. Therefore, the Amati relation obtained using external datasets as anchors, especially at high redshifts to break the circularity, may not always be robust for precision Cosmology. We should also point out that another caveat in using HII galaxy dataset as distance anchors is that there could be an evolution in the $L-\sigma$ between the low- and high-redshift samples [50]. This could also explain the large scatter, which we have observed in the Amati relation for the two datasets. Furthermore, one should also select a GRB dataset, which is standardizable [17–19] and independent of the underlying cosmological model, in order to make it suitable for cosmological analysis.

Table 1. Summary of our results for the Amati relation for A220 and D17 GRB datasets for z < 2.6. Both datasets show a high intrinsic scatter in the Amati relation

Dataset	a	b	$\sigma_{\!\scriptscriptstyle S}$
A220	0.54 ± 0.02	-25.42 ± 1.2	0.28 ± 0.013
D17	0.40 ± 0.03	-18.26 ± 1.8	0.35 ± 0.03

Universe **2025**, 1, 0 5 of 9

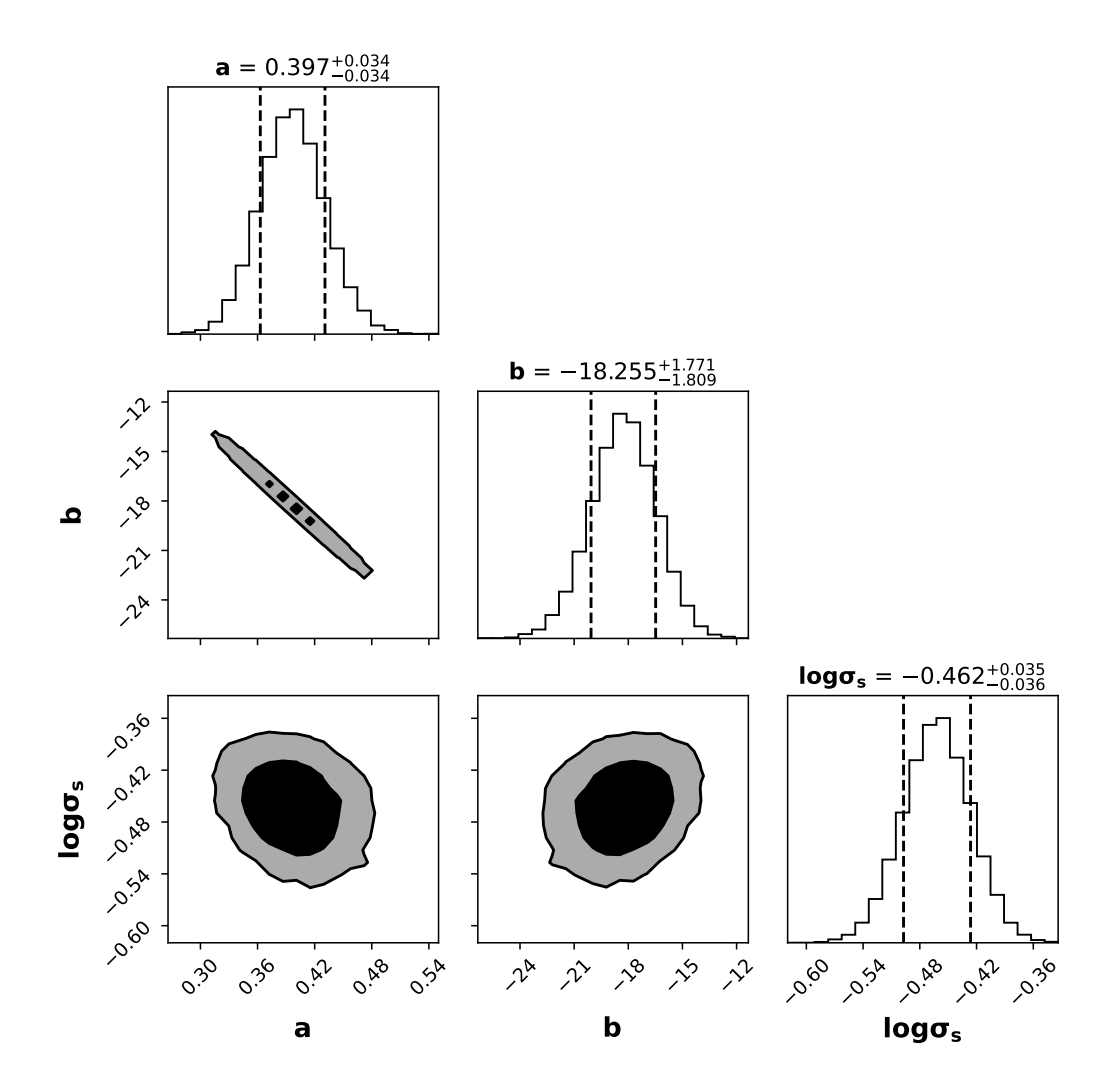


Figure 2. Marginalized 68% and 95% credible intervals for a, b, and $\ln \sigma_s$ (cf. Eq. 2) for the subset of D17 GRBs having z<2.6. The dashed vertical line in the marginalized plot shows the 68% uncertainty.

Universe **2025**, 1, 0 6 of 9

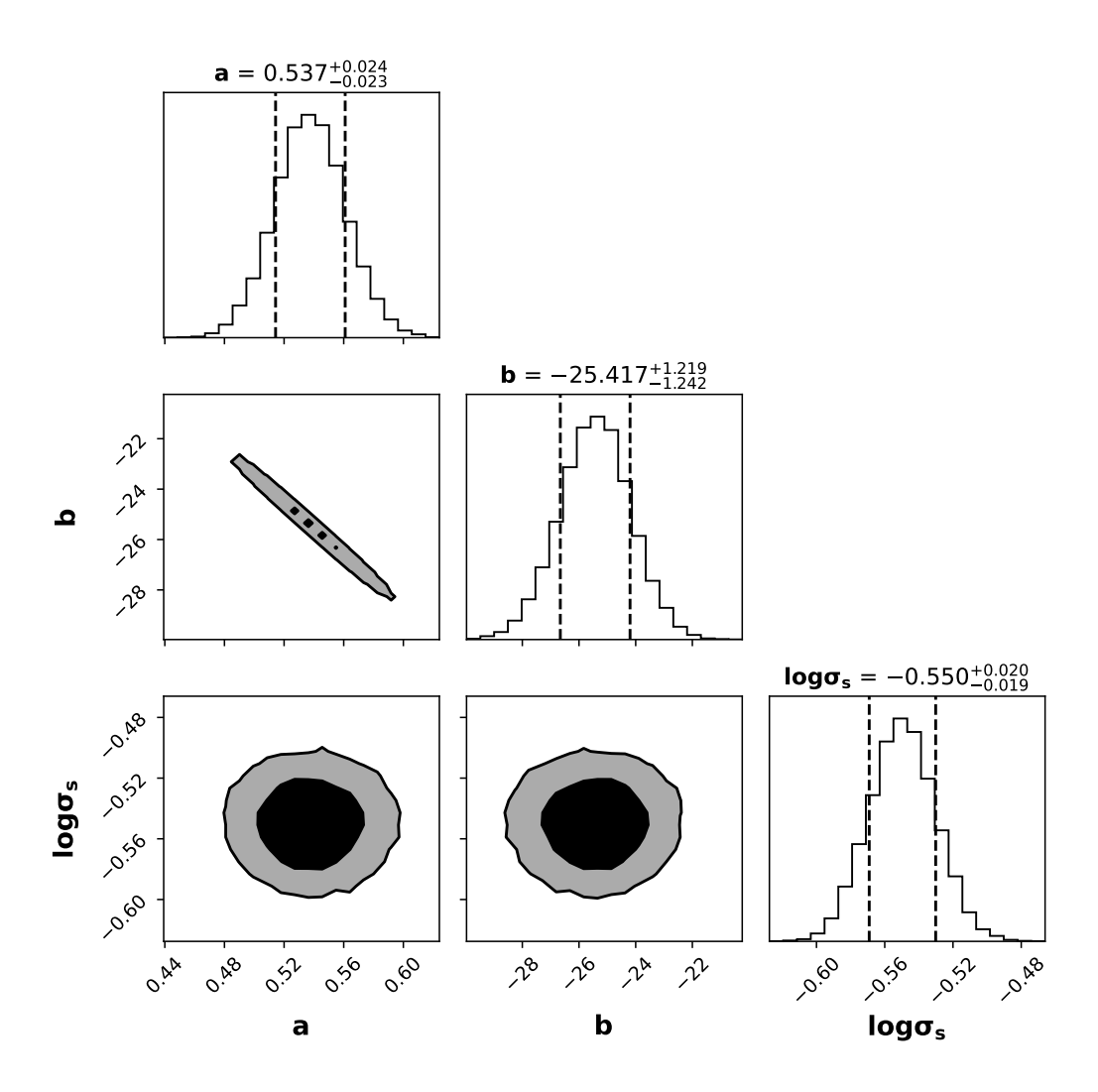


Figure 3. Marginalized 68% and 95% credible intervals for a, b, and $\ln \sigma_s$ (cf. Eq. 2) for the subset of A220 GRBs having z < 2.6. The dashed vertical line in the marginalized plot shows the 68% uncertainty.

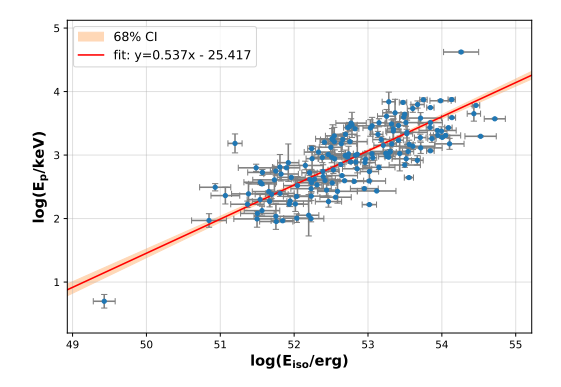


Figure 4. The best-fit regression line (red line) and the 1σ confidence interval (shaded region), derived from the MCMC posterior samples along with the data for A220 dataset having z < 2.6. The mean and standard deviation are computed at each x-coordinate from the ensemble of all posterior regression lines.

Universe **2025**, 1, 0 7 of 9

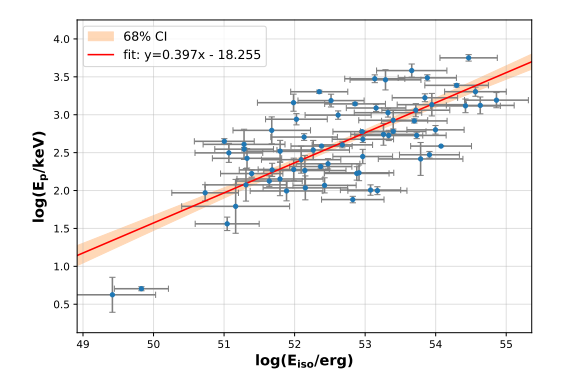


Figure 5. The best-fit regression line (red line) and the 1σ confidence interval (shaded region), derived from the MCMC posterior samples along with the data for D17 dataset having z < 2.6. The mean and standard deviation are computed at each x-coordinate from the ensemble of all posterior regression lines.

4. Conclusions

In this work, we have used 186 HII galaxy distances as anchors to calibrate the efficacy of the Amati relation between E_p and E_{iso} . We first used ANN based interpolation to reconstruct D_L for any GRB redshift. These interpolated values of D_L were used to obtain E_{iso} for the redshifts corresponding to two different GRB datasets (A220 and D17), which have previously been used for analysis of the Amati relation in a number of works, including G22.

We find that the best-fit parameters for both the datasets are consistent with the results for the same in G22 to within 1σ . However, the intrinsic scatter obtained for A220 and D17 is quite large, viz. 28% and 35%, respectively. Although this scatter is roughly comparable to the values obtained using other observables as distance anchors, it implies that the Amati relation using HII galaxies as distance anchors cannot be used for precision Cosmology.

Acknowledgments: RO would like to thank the JST Sakura Science Program (Grant No. M2025L0418003) and the JASSO Scholarship for supporting his travel to and stay at IIT Hyderabad. We also thank Yuva Himanshu Pallam for helping us to collate the HII galaxy dataset. We are grateful to the anonymous referees for several useful and constructive comments on our manuscript.

References

- 1. Kumar, P.; Zhang, B. The physics of gamma-ray bursts & relativistic jets. *Physics Reports* **2015**, *561*, 1–109, [arXiv:astro-ph.HE/1410.0679]. https://doi.org/10.1016/j.physrep.2014.09.008.
- 2. Kouveliotou, C.; Meegan, C.A.; Fishman, G.J.; Bhat, N.P.; Briggs, M.S.; Koshut, T.M.; Paciesas, W.S.; Pendleton, G.N. Identification of Two Classes of Gamma-Ray Bursts. *Astrophys. J. Lett.* **1993**, *413*, L101. https://doi.org/10.1086/186969.
- 3. Woosley, S.E.; Bloom, J.S. The Supernova Gamma-Ray Burst Connection. *Annual Review of Astron. and Astrophys.* **2006**, 44, 507–556, [arXiv:astro-ph/astro-ph/0609142]. https://doi.org/10.1146/annurev.astro.43.072103.150558.
- 4. Nakar, E. Short-hard gamma-ray bursts. *Physics Reports* **2007**, 442, 166–236, [arXiv:astro-ph/0701748]. https://doi.org/10.1016/j.physrep.2007.02.005.
- 5. Tsvetkova, A.; Amati, L.; Bulla, M.; Burderi, L.; Frederiks, D.; Frontera, F.; Guidorzi, C.; Riggio, A.; di Salvo, T.; Sanna, A.; et al. Gamma-ray burst taxonomy: Looking for the third class on the spectral peak energy-duration plane in the rest frame. *Astron. & Astrophys.* 2025, 698, A169, [arXiv:astro-ph.HE/2504.20263]. https://doi.org/10.1051/0004-6361/202452673.
- 6. Parsotan, T.; Ito, H. GRB Prompt Emission: Observed Correlations and Their Interpretations. *Universe* **2022**, *8*, 310, [arXiv:astro-ph.HE/2204.09729]. https://doi.org/10.3390/universe8060310.
- 7. Dainotti, M.G.; Del Vecchio, R. Gamma Ray Burst afterglow and prompt-afterglow relations: An overview. *New Astronomy Reviews* **2017**, 77, 23–61, [arXiv:astro-ph.HE/1703.06876]. https://doi.org/10.1016/j.newar.2017.04.001.
- 8. Dainotti, M.G.; Amati, L. Gamma-ray Burst Prompt Correlations: Selection and Instrumental Effects. *PASP* **2018**, *130*, 051001, [arXiv:astro-ph.HE/1704.00844]. https://doi.org/10.1088/1538-3873/aaa8d7.

Universe **2025**, 1, 0 8 of 9

9. Moresco, M.; Amati, L.; Amendola, L.; Birrer, S.; Blakeslee, J.P.; Cantiello, M.; Cimatti, A.; Darling, J.; Della Valle, M.; Fishbach, M.; et al. Unveiling the Universe with emerging cosmological probes. *Living Reviews in Relativity* **2022**, 25, 6, [arXiv:astro-ph.CO/2201.07241]. https://doi.org/10.1007/s41114-022-00040-z.

- 10. Luongo, O.; Muccino, M. A Roadmap to Gamma-Ray Bursts: New Developments and Applications to Cosmology. *Galaxies* **2021**, 9, 77, [arXiv:astro-ph.HE/2110.14408]. https://doi.org/10.3390/galaxies9040077.
- 11. Dainotti, M.G.; Nielson, V.; Sarracino, G.; Rinaldi, E.; Nagataki, S.; Capozziello, S.; Gnedin, O.Y.; Bargiacchi, G. Optical and X-ray GRB Fundamental Planes as cosmological distance indicators. *MNRAS* **2022**, *514*, 1828–1856, [arXiv:astro-ph.CO/2203.15538]. https://doi.org/10.1093/mnras/stac1141.
- 12. Bargiacchi, G.; Dainotti, M.G.; Capozziello, S. High-redshift cosmology by Gamma-Ray Bursts: An overview. *New Astronomy Reviews* **2025**, *100*, 101712, [arXiv:astro-ph.CO/2408.10707]. https://doi.org/10.1016/j.newar.2024.101712.
- 13. Amati, L.; Frontera, F.; Tavani, M.; in't Zand, J.J.M.; Antonelli, A.; Costa, E.; Feroci, M.; Guidorzi, C.; Heise, J.; Masetti, N.; et al. Intrinsic spectra and energetics of BeppoSAX Gamma-Ray Bursts with known redshifts. *Astron. & Astrophys.* **2002**, 390, 81–89, [arXiv:astro-ph/astro-ph/0205230]. https://doi.org/10.1051/0004-6361:20020722.
- 14. Amati, L. The $E_{p,i}$ - E_{iso} correlation in gamma-ray bursts: updated observational status, re-analysis and main implications. *MNRAS* **2006**, 372, 233–245, [arXiv:astro-ph/astro-ph/0601553]. https://doi.org/10.1111/j.1365-2966.2006.10840.x.
- 15. Collazzi, A.C.; Schaefer, B.E.; Goldstein, A.; Preece, R.D. A Significant Problem with Using the Amati Relation for Cosmological Purposes. *Astrophys. J.* **2012**, 747, 39, [arXiv:astro-ph.HE/1112.4347]. https://doi.org/10.1088/0004-637X/747/1/39.
- Amati, L.; Guidorzi, C.; Frontera, F.; Della Valle, M.; Finelli, F.; Landi, R.; Montanari, E. Measuring the cosmological parameters with the E_{p,i}-E_{iso} correlation of gamma-ray bursts. *MNRAS* 2008, 391, 577–584, [arXiv:astro-ph/0805.0377]. https://doi.org/10.1 111/j.1365-2966.2008.13943.x.
- 17. Khadka, N.; Ratra, B. Constraints on cosmological parameters from gamma-ray burst peak photon energy and bolometric fluence measurements and other data. *MNRAS* **2020**, *499*, 391–403, [arXiv:astro-ph.CO/2007.13907]. https://doi.org/10.1093/mnras/staa2779.
- 18. Khadka, N.; Luongo, O.; Muccino, M.; Ratra, B. Do gamma-ray burst measurements provide a useful test of cosmological models? *JCAP* 2021, 2021, 042, [arXiv:astro-ph.CO/2105.12692]. https://doi.org/10.1088/1475-7516/2021/09/042.
- 19. Cao, S.; Ratra, B. Testing the standardizability of, and deriving cosmological constraints from, a new Amati-correlated gamma-ray burst data compilation. *JCAP* **2024**, 2024, 093, [arXiv:astro-ph.CO/2404.08697]. https://doi.org/10.1088/1475-7516/2024/10/093.
- 20. Cao, S.; Ratra, B. Testing the consistency of new Amati-correlated gamma-ray burst dataset cosmological constraints with those from better-established cosmological data. *JCAP* **2025**, 2025, 081, [arXiv:astro-ph.CO/2502.08429]. https://doi.org/10.1088/1475 -7516/2025/09/081.
- 21. Liang, N.; Xiao, W.K.; Liu, Y.; Zhang, S.N. A Cosmology-Independent Calibration of Gamma-Ray Burst Luminosity Relations and the Hubble Diagram. *Astrophys. J.* **2008**, *685*, 354–360, [arXiv:astro-ph/0802.4262]. https://doi.org/10.1086/590903.
- 22. Liang, N.; Li, Z.; Xie, X.; Wu, P. Calibrating Gamma-Ray Bursts by Using a Gaussian Process with Type Ia Supernovae. *Astrophys. J.* 2022, 941, 84, [arXiv:astro-ph.CO/2211.02473]. https://doi.org/10.3847/1538-4357/aca08a.
- 23. Kodama, Y.; Yonetoku, D.; Murakami, T.; Tanabe, S.; Tsutsui, R.; Nakamura, T. Gamma-ray bursts in 1.8 < z < 5.6 suggest that the time variation of the dark energy is small. *MNRAS* **2008**, *391*, L1–L4, [arXiv:astro-ph/0802.3428]. https://doi.org/10.1111/j.1745 -3933.2008.00508.x.
- 24. Demianski, M.; Piedipalumbo, E.; Sawant, D.; Amati, L. Cosmology with gamma-ray bursts. I. The Hubble diagram through the calibrated E_{p,I}-E_{iso} correlation. *Astron. & Astrophys.* **2017**, *598*, A112, [arXiv:astro-ph.CO/1610.00854]. https://doi.org/10.1051/0004-6361/201628909.
- 25. Liu, Y.; Liang, N.; Xie, X.; Yuan, Z.; Yu, H.; Wu, P. Gamma-Ray Burst Constraints on Cosmological Models from the Improved Amati Correlation. *Astrophys. J.* **2022**, *935*, 7, [arXiv:astro-ph.CO/2207.00455]. https://doi.org/10.3847/1538-4357/ac7de5.
- 26. Huang, Z.; Luo, X.; Zhang, B.; Feng, J.; Wu, P.; Liu, Y.; Liang, N. Gamma-Ray Bursts Calibrated by Using Artificial Neural Networks from the Pantheon+ Sample. *Universe* **2025**, *11*, 241, [arXiv:astro-ph.CO/2506.08929]. https://doi.org/10.3390/universe11080241.
- 27. Montiel, A.; Cabrera, J.I.; Hidalgo, J.C. Improving sampling and calibration of gamma-ray bursts as distance indicators. *MNRAS* **2021**, 501, 3515–3526, [arXiv:astro-ph.HE/2003.03387]. https://doi.org/10.1093/mnras/staa3926.
- 28. Amati, L.; D'Agostino, R.; Luongo, O.; Muccino, M.; Tantalo, M. Addressing the circularity problem in the E_p - E_{iso} correlation of gamma-ray bursts. *MNRAS* **2019**, *486*, L46–L51, [arXiv:astro-ph.HE/1811.08934]. https://doi.org/10.1093/mnrasl/slz056.
- 29. Luongo, O.; Muccino, M. Model-independent calibrations of gamma-ray bursts using machine learning. *MNRAS* **2021**, 503, 4581–4600, [arXiv:astro-ph.CO/2011.13590]. https://doi.org/10.1093/mnras/stab795.
- 30. Luongo, O.; Muccino, M. Intermediate redshift calibration of Gamma-ray Bursts and cosmic constraints in non-flat cosmology. *arXiv e-prints* **2022**, p. arXiv:2207.00440, [arXiv:astro-ph.CO/2207.00440].
- 31. Kumar, D.; Rani, N.; Jain, D.; Mahajan, S.; Mukherjee, A. Gamma rays bursts: a viable cosmological probe? *JCAP* **2023**, 2023, 021, [arXiv:astro-ph.CO/2212.05731]. https://doi.org/10.1088/1475-7516/2023/07/021.

Universe **2025**, 1, 0 9 of 9

32. Wang, H.; Liang, N. Constraints from Fermi observations of long gamma-ray bursts on cosmological parameters. *MNRAS* **2024**, 533, 743–755, [arXiv:astro-ph.CO/2405.14357]. https://doi.org/10.1093/mnras/stae1825.

- 33. Huang, Z.; Xiong, Z.; Luo, X.; Wang, G.; Liu, Y.; Liang, N. Gamma-ray bursts calibrated from the observational H(z) data in artificial neural network framework. *Journal of High Energy Astrophysics* **2025**, 47, 100377, [arXiv:astro-ph.CO/2502.10037]. https://doi.org/10.1016/j.jheap.2025.100377.
- 34. Govindaraj, G.; Desai, S. Low redshift calibration of the Amati relation using galaxy clusters. *JCAP* **2022**, 2022, 069, [arXiv:astro-ph.HE/2208.00895]. https://doi.org/10.1088/1475-7516/2022/10/069.
- 35. Dai, Y.; Zheng, X.G.; Li, Z.X.; Gao, H.; Zhu, Z.H. Redshift evolution of the Amati relation: Calibrated results from the Hubble diagram of quasars at high redshifts. *Astron. & Astrophys.* **2021**, *651*, L8, [arXiv:astro-ph.HE/2111.05544]. https://doi.org/10.1051/0004-6361/202140895.
- 36. Terlevich, R.; Melnick, J. The dynamics and chemical composition of giant extragalactic H II regions. *MNRAS* **1981**, *195*, 839–851. https://doi.org/10.1093/mnras/195.4.839.
- 37. Siegel, E.R.; Guzmán, R.; Gallego, J.P.; Orduña López, M.; Rodríguez Hidalgo, P. Towards a precision cosmology from starburst galaxies at z > 2. *MNRAS* 2005, 356, 1117–1122, [arXiv:astro-ph/astro-ph/0410612]. https://doi.org/10.1111/j.1365-2966.2004.0 8539.x.
- 38. Chávez, R.; Terlevich, E.; Terlevich, R.; Plionis, M.; Bresolin, F.; Basilakos, S.; Melnick, J. Determining the Hubble constant using giant extragalactic H II regions and H II galaxies. *MNRAS* **2012**, 425, L56–L60, [arXiv:astro-ph.CO/1203.6222]. https://doi.org/10.1111/j.1745-3933.2012.01299.x.
- 39. Mania, D.; Ratra, B. Constraints on dark energy from H II starburst galaxy apparent magnitude versus redshift data. *Physics Letters B* **2012**, 715, 9–14, [arXiv:astro-ph.CO/1110.5626]. https://doi.org/10.1016/j.physletb.2012.07.011.
- 40. Wei, J.J.; Melia, F. Model selection using the HII galaxy Hubble diagram. MNRAS 2025, 542, L19–L23, [arXiv:astro-ph.CO/2506.04819]. https://doi.org/10.1093/mnrasl/slaf060.
- 41. Zheng, J.; Qiang, D.C.; You, Z.Q.; Kumar, D. Quantifying the Impact of 2D and 3D BAO Measurements on the Cosmic Distance Duality Relation with HII Galaxy observation. *arXiv e-prints* **2025**, p. arXiv:2507.17113, [arXiv:astro-ph.CO/2507.17113]. https://doi.org/10.48550/arXiv.2507.17113.
- 42. Demianski, M.; Piedipalumbo, E.; Sawant, D.; Amati, L. Cosmology with gamma-ray bursts. II. Cosmography challenges and cosmological scenarios for the accelerated Universe. *Astron. & Astrophys.* **2017**, *598*, A113, [arXiv:astro-ph.CO/1609.09631]. https://doi.org/10.1051/0004-6361/201628911.
- 43. González-Morán, A.L.; Chávez, R.; Terlevich, E.; Terlevich, R.; Fernández-Arenas, D.; Bresolin, F.; Plionis, M.; Melnick, J.; Basilakos, S.; Telles, E. Independent cosmological constraints from high-z H II galaxies: new results from VLT-KMOS data. *MNRAS* **2021**, *505*, 1441–1457, [arXiv:astro-ph.CO/2105.04025]. https://doi.org/10.1093/mnras/stab1385.
- 44. Llerena, M.; Amorín, R.; Pentericci, L.; Calabrò, A.; Shapley, A.E.; Boutsia, K.; Pérez-Montero, E.; Vílchez, J.M.; Nakajima, K. Ionized gas kinematics and chemical abundances of low-mass star-forming galaxies at z ~ 3. *Astron. & Astrophys.* **2023**, *676*, A53, [arXiv:astro-ph.GA/2303.01536]. https://doi.org/10.1051/0004-6361/202346232.
- 45. de Graaff, A.; Rix, H.W.; Carniani, S.; Suess, K.A.; Charlot, S.; Curtis-Lake, E.; Arribas, S.; Baker, W.M.; Boyett, K.; Bunker, A.J.; et al. Ionised gas kinematics and dynamical masses of z ≥ 6 galaxies from JADES/NIRSpec high-resolution spectroscopy. *Astron. & Astrophys.* **2024**, *684*, A87, [arXiv:astro-ph.GA/2308.09742]. https://doi.org/10.1051/0004-6361/202347755.
- 46. Ball, N.M.; Brunner, R.J. Data Mining and Machine Learning in Astronomy. *International Journal of Modern Physics D* **2010**, 19, 1049–1106, [arXiv:astro-ph.IM/0906.2173]. https://doi.org/10.1142/S0218271810017160.
- 47. Efron, B.; Tibshirani, R.J. An introduction to the bootstrap; Chapman & Hall/CRC, 1993.
- 48. Foreman-Mackey, D.; Hogg, D.W.; Lang, D.; Goodman, J. emcee: The MCMC Hammer. *Publ. Astron. Soc. Pac.* **2013**, 125, 306–312, [arXiv:astro-ph.IM/1202.3665]. https://doi.org/10.1086/670067.
- 49. Liu, Y.; Chen, F.; Liang, N.; Yuan, Z.; Yu, H.; Wu, P. The Improved Amati Correlations from Gaussian Copula. *Astrophys. J.* **2022**, 931, 50, [arXiv:astro-ph.CO/2203.03178]. https://doi.org/10.3847/1538-4357/ac66d3.
- 50. Cao, S.; Ratra, B. Low- and high-redshift H II starburst galaxies obey different luminosity-velocity dispersion relations. *Physical Review D.* **2024**, 109, 123527, [arXiv:astro-ph.CO/2310.15812]. https://doi.org/10.1103/PhysRevD.109.123527.

Appendix

Disclaimer/Publisher's Note: The statements, opinions and data contained in all publications are solely those of the individual author(s) and contributor(s) and not of MDPI and/or the editor(s). MDPI and/or the editor(s) disclaim responsibility for any injury to people or property resulting from any ideas, methods, instructions or products referred to in the content.